Photomodulation of Kv Channel Activity

Rohit Yadav[1,a], Juergen Pfeffermann[1,a], Nikolaus Goessweiner-Mohr[1], Toma Glasnov[2], Sergey A. Akimov[3], Peter Pohl[1,*]

[1]Institute of Biophysics, Johannes Kepler University Linz, Linz, Austria

[2]Institute of Chemistry, Karl-Franzens-University, Graz, Austria

[3]Frumkin Institute of Physical Chemistry and Electrochemistry,

Russian Academy of Sciences, Moscow, Russia

[a]These authors contributed equally

*Correspondence to: peter.pohl@jku.at

Voltage-gated potassium (Kv) channels, essential for shaping action potentials, are influenced not only by voltage but also by mechanical stimuli. Membrane tension has been shown to stabilize the open state of the pore, suggesting that pore dilation occurs in a thinner membrane. However, structural studies using cryo-electron microscopy indicate that membrane thinning is associated with pore closure. To clarify the role of local hydrophobic membrane thickness in channel gating, we reconstituted Kv channels from *Aeropyrum pernix* (KvAP) into planar bilayers containing photoswitchable lipids. Blue light exposure increased membrane thickness and increased the KvAP activity at both single channel and ensemble levels, whereas UV light reversed these effects by decreasing thickness and reducing activity. These results support a model in which the positioning of lipid phosphates in a thicker membrane drives the upward movement of interacting arginine residues in the KvAP voltage sensor and primes the channel for opening. This light-driven regulation of Kv channel activity offers new possibilities for controlling neuronal excitability.

Introduction

Voltage-gated ion channels enable rapid cellular excitability, particularly within neuronal systems. Among them, voltage-gated potassium ion (Kv) channels play a crucial role in regulating the shape and duration of action potentials.[1,2] Kv channels are tetrameric complexes, each subunit containing a voltage-sensing domain (VSD) formed by four transmembrane segments (S1–S4) arranged around a central conducting pore domain composed of two transmembrane helices (S5 and S6) contributed by each subunit.[3]

Kv channels respond to changes in membrane voltage by conformational changes,[4] enabling pore opening and closing through the movement of positively-charged amino acid residues in S4, known as gating charges.[5,6] Due to these gating charges, VSDs exhibit pronounced interactions with the surrounding phospholipid headgroups, which can induce local deformations in the lipid membrane that may influence channel function.[7-10] Such lipid bilayer deformations have been extensively studied and characterized,[7,9-11] revealing the critical role of the lipid bilayer in modulating channel function and dynamics.

Recent cryo-electron microscopy studies of Kv channel-containing vesicles at different membrane potentials have provided structural insights into the conformational transitions associated with channel closing in the mammalian non-domain-swapped Kv channel Eag.[12] These studies revealed that the closed channel is situated in a region of the membrane approximately 5 Å thinner than its surroundings, suggesting a relationship between membrane thickness and channel conformation.

Cholesterol, known for its membrane-thickening effects,[13] was also shown to modulate the activity of another non-domain-swapped channel, the Kv channel from *Aeropyrum pernix* (KvAP).[14] Based on the observed interplay between membrane thickness and channel state in the Eag channel,[12] it might be expected that cholesterol addition would increase KvAP's activity by stabilizing an open-state conformation. Surprisingly, cholesterol instead induced inactivation.[14]

Interestingly, Kv channels are sensitive to membrane tension.[15] One proposed explanation is that membrane tension favors a state of the protein with an increased cross-sectional area within the membrane plane. For this to occur, the protein must be as or more compliant to tension than the lipid bilayer, which has an area expansion modulus of approximately 250 mN/m.[16] However, data on the area expansion modulus of proteins remain scarce, and existing theoretical models for mechanosensitive channels do not support the idea that protein expansion in response to tension may act as the exclusive gating stimulus. For the mechanosensitive Piezo channels a dome model was proposed where tension

flattens the initially curved membrane leading to channel opening.[17] This transformation is plausible because the bending stiffnesses of the channel and bilayer are comparable.[18] Similarly, the gating of the mechanosensitive channel MscL has been linked to changes in membrane thickness. In this case, the hydrophobic mismatch between the membrane protein and surrounding lipids generates line tension, which plays a crucial role in channel gating.[19]

KvAP has been described to induce membrane curvature,[20] but whether channel activation alters membrane curvature has not been shown. Moreover, an adaptation of Piezo's dome model would be questionable, as the channel area of KvAP is much smaller and much less infiltrated with lipids; hence, its bending modulus is unlikely to be as lipid-like as that of Piezo.[18]

The counterintuitive combination of activation by membrane tension[15] and deactivation by membrane thinning[12] raises an intriguing question: would a mere change in bilayer thickness tend to increase KvAP channel activity? To address this question, we employed photoswitchable lipids in our study. However, their application must be approached with caution, given the complex interplay between the VSDs of Kv channels and the lipid bilayer's composition and mechanics.[7,9] For instance, the gating of KvAP is highly sensitive to the lipid composition of the surrounding bilayer. The presence of non-phospholipids has been shown to impair channel activation by voltage, while variations in lipid shape significantly influence voltage-dependent behavior.[21] Additionally, enzymatic hydrolysis of the head group in sphingomyelin was reported to inhibit the activity of Kv2.1 channels, further highlighting the critical role of lipid head groups for Kv channel function.[22] Furthermore, the addition of alkanols within specific molar ranges, which alters bilayer mechanics, also affects KvAP conductance and activation kinetics.[23]

We conclude that the precise mechanisms by which membrane lipids modulate Kv function remain incompletely understood. To address this, a well-defined artificial system is needed – one that allows isolation of specific channels of interest and precise control over membrane thickness.

To address the above, we adopted an optically excited photolipid-based approach using photolipids in solvent-depleted planar lipid bilayers (PLBs). Specifically, we utilized azobenzene-containing diacylglycerols (OptoDArG) which undergo rapid and reversible photoisomerization upon exposure to UV (375 nm) or blue (488 nm) light. The photoisomerization of membrane-embedded OptoDArG reversibly alters mechanical properties of the lipid bilayer.[24,25] Recently, we demonstrated that this rapid photoisomerization can induce changes in membrane capacitance on the millisecond timescale, generating optocapacitive currents that lead to membrane de- or hyperpolarization in response to light.[26]

Blue light (cis to trans state) evoked hyperpolarizing optocapacitive currents by reducing the area per photolipid molecule, which was accompanied by membrane thickening and the activation of mechanosensitive channels in the plasma membrane. Our intuitive interpretation was that the rapid reduction in area per lipid upon transitioning from cis to trans photoisomers by blue light irradiation generates membrane tension, σ. Alternatively, endogenous mechanosensitive channels may have responded to isomerization-induced changes in membrane thickness,[24,27] spontaneous curvature,[25,28] or bending rigidity[29].

In this study, we first estimated the amount of σ generated by photolipid switching by imaging the movement of the anchored solvent annulus (torus) in photoswitchable PLBs, alongside with high-frequency recordings of membrane capacitance. Subsequently, we reconstituted KvAP, a model Kv channel with a non-domain-swapped voltage sensor, into solvent-depleted PLBs containing ≈20 m% photoswitchable lipids. We successfully modulated KvAP activity through the photoisomerization of OptoDArG between cis and trans conformations. This approach enabled us to identify membrane thickness as a key factor in KvAP gating.

Results

Fast photoisomerization of OptoDArG generates only a small transient increment in membrane tension

To investigate whether photolipid isomerization significantly augments membrane tension (σ), we folded planar lipid bilayers (PLBs) with a prominent anchoring solvent-annulus (Fig. 1a). While typically minimized to reduce residual solvent[30] (yellow in Fig. 1e), the larger annuli in our experiments enabled visualization of the torus's inward deformation under intense blue light (Fig. 1b). Initially, UV light induced the cis state of the bilayer, characterized by finite membrane tension, σ_0, and capacitance, C_m (**1** in Fig. 1c-d). Upon equilibrium, blue light exposure triggered cis-to-trans photoisomerization, leading to a rapid reduction in bilayer area (A_m, Supplementary Video). This increased σ, resulting in a reshaped torus (Fig. 1e). The origin of σ is trans-OptoDArG's smaller molecular area compared to its cis counterpart (Fig. 1f).

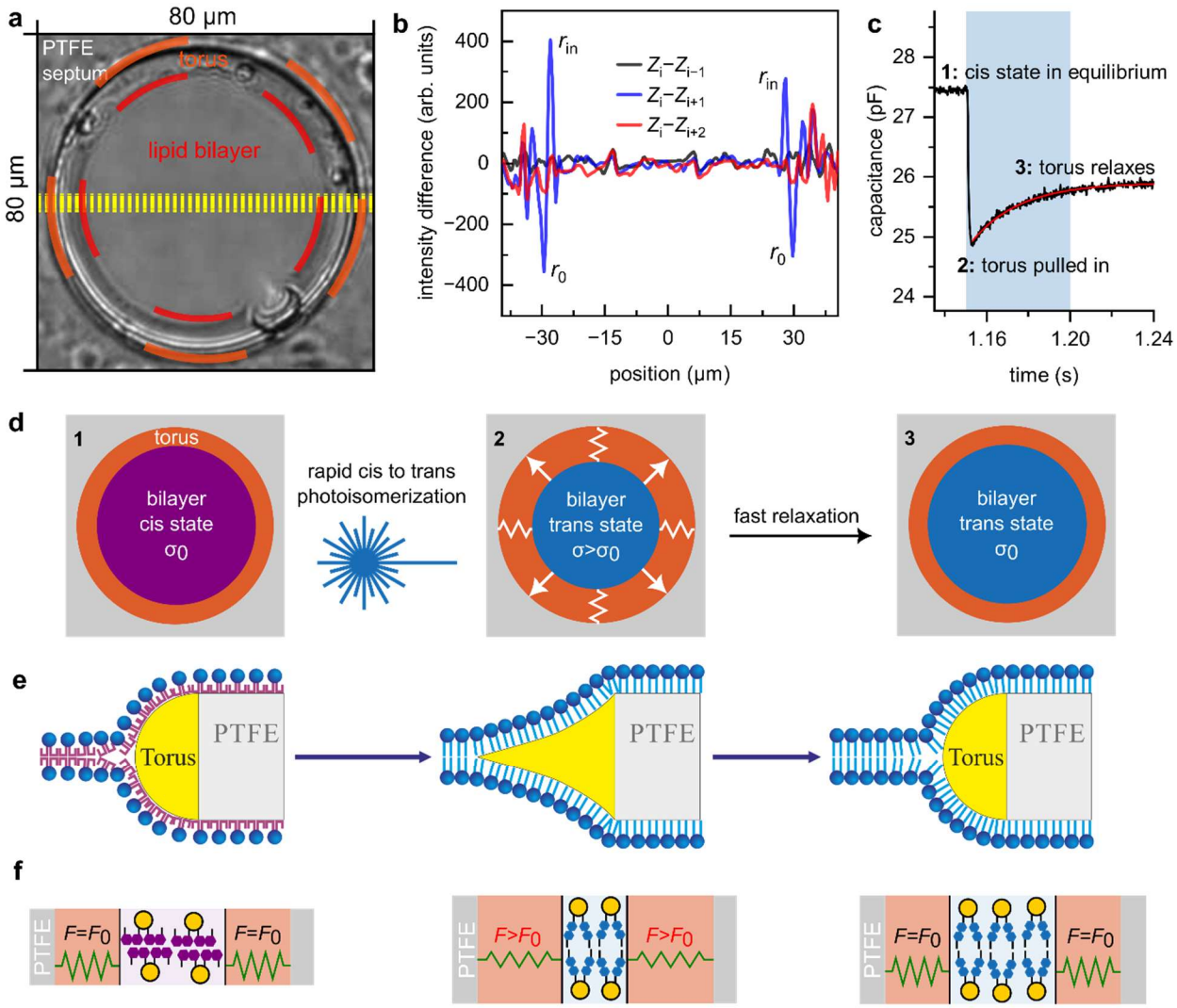

Figure 1|a, A transmitted light image of a photoswitchable PLB with an enforced large torus. Lipid bilayer, torus and PTFE septum are indicated. **b,** Z_i corresponds to the average line profile (obtained from the yellow dashed lines in panel **a** of frame i immediately before blue light exposure, Z_{i-1} the line profile of the frame before, Z_{i+1} and Z_{i+2} the average line profiles corresponding to one and two frames after frame i, respectively. The calculated differences demonstrate the inwards movement of the torus following blue light exposure ($Z_i - Z_{i+1}$, blue line) and the return to the initial shape one frame later ($Z_i - Z_{i+2}$, red line). The lines are averaged from seven switching events on the same PLB. **c,** Time course of C_m upon blue light exposure (indicated by the blue background) of a cis-OptoDArG containing PLB. C_m decreases rapidly as photolipids switch to the trans state and the torus is pulled inwards; subsequently, C_m relaxes, which is partially due to the increase in A_m as the torus retracts again. The red line is a monoexponential fit to the relaxation. **d,** Schematic view of the response of a photoswitchable PLB to blue light irradiance. σ may be increased transiently as the torus is stretched by the bilayer. As described below, σ relaxes within 80 ms. **e,** Schematic representation of torus shape corresponding to the bilayer states in panel **d**. **f,** Schematics of how

photoisomerization from cis- to trans-OptoDArG generates tension within the membrane. The grey bars labeled PTFE symbolize the septum aperture within which the PLB is mounted, and green springs refer to the bilayer lipids other than OptoDArG.

A rough estimation of σ can be made from the observed radius change. Immediately after blue light exposure, the radius of the bilayer in the middle of the toroidal reservoir decreases from r_0= 29.5 µm to r_{in} = 27.5 µm (Fig. 1b) before quickly relaxing to its initial value (within one frame). Importantly, key parameters depend on $\ln(r_0/r_{in})$, making the exact values less critical. Denoting the equilibrium lateral tension of the membrane at r_0 as σ_0 and the tension at r_{in} as $\sigma_0(1 + \alpha)$, we assume that the lateral tension evolves linearly with time, t, during the relaxation ($0 < t < \tau$). Thus, $\sigma(t) = At + B$, with boundary conditions $\sigma(0) = \sigma_0(1 + \alpha)$ and $\sigma(\tau) = \sigma_0$, allowing us to determine A and B as $A = -\alpha\sigma_0/\tau$ and $B = \sigma_0(1 + \alpha)$.

The radial flow of viscous lipid follows the equation[31]:

$$4\pi\eta h\dot{r} = 2\pi r\sigma \tag{1}$$

where η is the surface viscosity (membrane viscosity times membrane thickness). When $\sigma = \sigma_0$, the membrane rim is in equilibrium (i.e., no motion occurs). Substituting $\sigma(t) - \sigma_0 = \alpha\sigma_0 (1 - t/\tau)$ into Eq. 1 and solving for $r(t)$ with boundary conditions $r(0) = r_{in}$ and $r(\tau) = r_0$ yields the solution:

$$r(t) = r_{in} \exp\left[ln\left(\frac{r_0}{r_{in}}\right)\frac{(2\tau - t)t}{\tau^2}\right] \tag{2}$$

Notably, $r(t)$ changes exponentially, as do A_m and C_m (Fig. 1c), supporting the assumption of a linear dependence of σ on t. To estimate τ, we need to estimate the rate at which σ decays following blue light exposure. To that effect, we obtained consistent results from imaging and C_m measurements:

1. From the video recordings, we quantified the torus movement by averaging 11 line profiles along the equator of the PLB (yellow lines, Fig. 1a), resulting in an average profile Z_i for each frame i. For seven instances of cis-to-trans photoisomerization (see Supplementary Video), we selected Z_i just before light exposure and verified that it was indistinguishable from the previous profile Z_{i-1} by calculating the difference $Z_i - Z_{i-1}$ (black line in Fig. 1b). Following blue light exposure, $Z_i - Z_{i+1}$ (blue line in Fig. 1b) displayed pronounced positive (r_{in}) and negative (r_0) deflections, indicating inward torus movement from r_0 to r_{in}. Finally, $Z_i - Z_{i+2}$ (red line in 1b) no longer exhibited these peaks, showing that the torus relaxes within less than twice the frame interval of 40 ms, i.e., $\tau < 80$ ms.

2. The rate of decrease in C_m at the onset of blue light exposure is rapid and largely determined by irradiance and azobenzene photoisomerization kinetics.[26] C_m reaches a minimum as OptoDArG is quantitatively photoisomerized (**2** in Fig. 1c), resulting in bilayer thickening and a reduction in A_m as the torus is pulled inwards. Then, C_m relaxes with an estimated time constant $\tau \approx 23$ ms (monoexponential fit to the relaxation in C_m; red line in Fig. 1c). This increase in C_m is consistent with the observed increase in A_m as the torus retracts. Hence, we conclude that the relaxation in torus position and C_m reflect the same underlying phenomenon.

With the above determined values r_0 = 29.5 µm, r_{in} = 27.5 µm, and τ = 23 ms and assuming the tension of a planar bilayer to be $\sigma_0 \approx 4$ mN/m,[32] we can find α by solving Eq. 2 with the boundary conditions imposed above on $r(t)$:

$$\alpha = 4\, ln\left(\frac{r_0}{r_{in}}\right)\frac{\eta h}{\sigma_0 \tau} \tag{3}$$

For solvent-depleted PLBs we previously measured ηh = 4 nNs/m.[33] Substituting this value into Eq. 3 yields an increment in σ of 0.001 %. Yet, estimates for ηh vary considerably – typically between 0.15 and 15 nNs/m.[34] For lipid domains, values as high as 500 nNs/m have been reported.[35] Using this upper value, we estimate α≈0.15%, suggesting that the tension could increase from 4 to 4.006 mN/m. However, there is no previous evidence indicating that Kv channels can respond measurably to such tiny changes in tension.

Functional reconstitution of KvAP into solvent-depleted PLBs containing OptoDArG

KvAP was expressed in *Escherichia coli* and purified following a protocol previously established for the bacterial K^+ channel KcsA.[36] Extraction from the cell pellet using n-dodecyl-β-D-maltoside (DDM) was validated via size-exclusion chromatography (SEC) and SDS-PAGE analysis. The SEC chromatogram exhibited a peak at an elution volume of 11 mL, consistent with the expected size of tetrameric KvAP [e.g., ref. [37]]. SDS-PAGE further confirmed the tetrameric assembly of the channel in detergent micelles (Fig. 2a).

Subsequently, DDM was replaced with *E. coli* polar lipid extract (PLE), forming vesicles that incorporated KvAP into their membranes. These vesicles were fused with solvent-depleted planar lipid bilayers (PLBs) composed of PLE (specific capacitance ≥ 0.75 µF/cm²) containing 0 or 20 m% OptoDArG. Fusion was driven

by a 150 to 15 mM KCl gradient.[36] This method facilitated the study of single-channel and ensemble currents by varying the protein-to-lipid ratio.

The single-channel conductance of KvAP (Fig. 2d) recorded in photoswitchable PLBs containing 20 m% trans-OptoDArG in 150 mM KCl was determined to be 190±6 pS, based on the single-channel current/voltage (I/V) relationship (see Supplementary Figure). This value closely aligns with previously reported conductance measurements.[38] To assess the functionality of KvAP in macroscopic currents, we fused proteoliposomes containing a high protein-to-lipid ratio in PLBs, both with and without OptoDArG. Under both conditions, KvAP exhibited robust voltage-dependent gating (Fig. 2b, c, e). Channel activity was inhibited by 0.4 µM of charybdotoxin (CTX), a known pore blocker of KvAP (Fig. 2c). This inhibition follows a key-lock mechanism, as described in previous studies.[38-40] Voltage-dependent activation and CTX-mediated inhibition confirm the successful reconstitution of functional KvAP channels into photoswitchable PLBs.

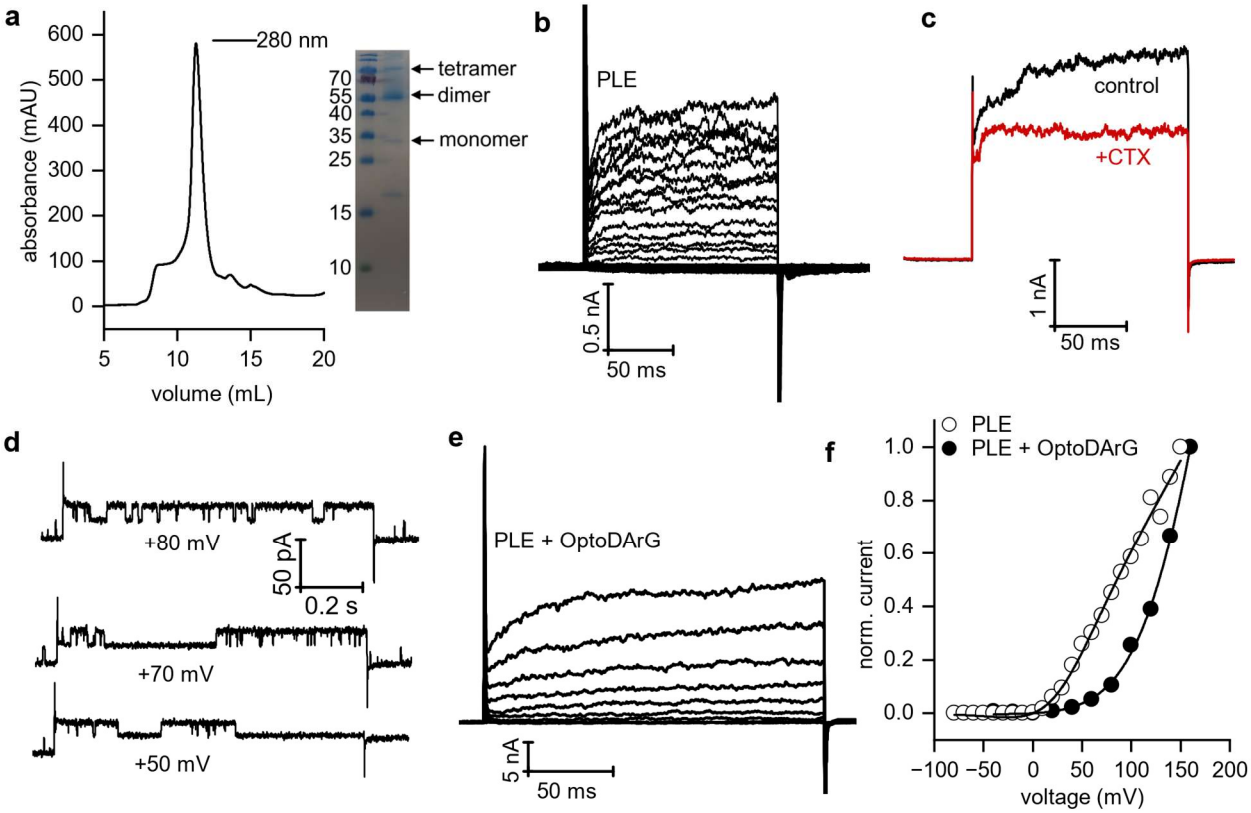

Figure 2|Functional reconstitution of KvAP into solvent-depleted PLBs. a, (Left) Size-exclusion chromatogram showing a peak at 11 mL, corresponding to KvAP. (Right) SDS-PAGE analysis confirming KvAP tetramers in detergent micelles. **b,** Voltage-clamp current recordings on a solvent-depleted PLB containing reconstituted KvAP channels. Voltage pulses were applied from −80 mV to +150 mV in 10 mV increments, with a holding potential (h.p.) of −100 mV and 5 s inter-sweep delays. **c,** Inhibition of KvAP by 0.4 µM CTX. Currents were recorded during voltage pulses from −80 mV to +100 mV, with an h.p. of −100 mV. **d**, Single-channel recordings of KvAP in photoswitchable PLBs. **e**, Current recordings from a photoswitchable PLB. Voltage pulses were applied from −40 mV to +160 mV in 20 mV increments, with a h.p. of −100 mV and 5 s inter-sweep delays. **f**, Normalized I/V curves constructed from the records shown in **b** (open circles) and **e** (closed circles), fitted using Eq. 4. Panels **b-f:** PLBs were folded from PLE with 20 m% trans-OptoDArG in 150 mM KCl, 10 mM HEPES, pH 7.4.

Voltage-dependent gating of KvAP is influenced by solvent content and the presence of non-phospholipids

I/V curves derived from ensemble recordings in the absence (Fig. 2b) and presence of trans-OptoDArG (Fig. 2e) were fitted using a Boltzmann equation:[41]

$$I(V) = \frac{(V - V_{\mathrm{rev}}) \times G_{\mathrm{max}}}{1 + \exp\left(\frac{V - V_{1/2}}{V_{\mathrm{s}}}\right)} \tag{4}$$

where V represents voltage, and the parameters V_{rev}, G_{max}, $V_{1/2}$, and V_s correspond to the reversal potential, maximum conductance, half-maximal activation voltage, and slope factor, respectively.

In PLBs composed of PLE, a pronounced depolarizing shift in $V_{1/2}$ to 28±5 mV (Fig. 2b, f) was observed compared to earlier studies using black lipid membranes (BLMs) painted from 1:3 POPE:POPG in *n*-decane, where $V_{1/2}$ was −51mV.[38] This shift likely arises from decane retained between the leaflets in BLMs, which is also reflected in their lower specific capacitance compared to PLBs. Our findings align with prior studies [21,42] showing a large difference in $V_{1/2}$ for Kv1.2 channels, transitioning from −70 mV in BLMs to −3.5 mV in oocytes. Similarly, KvAP studies in other solvent-free systems, such as giant unilamellar vesicles (GUVs)[37] and bead-supported unilamellar membranes (bSUMs)[43], also revealed a positive shift in voltage activation.

Furthermore, the incorporation of 20 m% trans-OptoDArG into the PLBs produced an additional rightward shift in $V_{1/2}$ (Fig. 2f). This indicates that 20 m% of the non-phospholipid OptoDArG (a diacylglycerol) modulates KvAP activation, emphasizing the necessity of phosphate groups for Kv gating.[8] Additionally, we observed that channel activation kinetics in PLBs were slower and that inactivation was incomplete

compared to BLMs (Fig. 2e). These characteristics are consistent with other studies of Kv channels, including the paddle chimera and KvAP, in solvent-free bilayers such as oocytes, GUVs, and bSUMs.[21,44,45]

In summary, our results demonstrate that residual solvent in BLMs influences both the voltage activation and kinetic properties of Kv channels. They underscore the impact of membrane mechanics and composition – particularly the presence of non-phospholipids and solvent-free conditions – on Kv channel gating.

Rapid photoisomerization of membrane-embedded OptoDArG gates KvAP

Following the functional characterization of KvAP in PLBs, we investigated how changes in thickness influence KvAP gating. Single-channel activity of KvAP was modulated by the photoisomerization of OptoDArG (Fig. 3a). Experiments began with a 40 ms UV light pulse, converting all OptoDArG molecules into their cis configuration. This transition reduced membrane thickness, leading to an increase in membrane capacitance (C_m).[26] The associated optocapacitive current was characterized by a rapid, transient depolarizing peak, followed by a activity decrease of KvAP channels (Fig. 3a, b, c). We observed that the number of active channels was different in cis and trans bilayers. In other words, determining the open probability of a channel from the fraction of its open time in a cis bilayer can be misleading because channels that were electrically silent become active after photoswitching to the trans bilayer. Therefore, in our recordings where individual channels are visible, we use the term open probability P_o to describe the probability of finding at least one channel in the open state. Obviously, this term is not applicable to ensemble measurements.

Subsequent illumination with a 40 ms blue light pulse induced the reversible isomerization of OptoDArG to the trans conformation. This transition decreased C_m and the area per photolipid (Fig. 1), resulting in a persistent increase in membrane thickness. The thicker membrane favored KvAP channel openings, as indicated by a higher P_o (Fig. 3a, b, c).

Exposure to a second UV light pulse reduced KvAP channel activity again, confirming the reversible modulation of KvAP gating by photolipid photoisomerization and the associated changes in bilayer properties. Importantly, no significant difference in KvAP single-channel conductance was observed between cis- and trans-OptoDArG states; in both cases, the conductance value agreed with measurements in the absence of OptoDArG.

Control experiments without KvAP channels demonstrated that UV and blue light elicited optocapacitive currents without affecting bilayer permeability (Fig. 3a), thereby ruling out photolipid-induced artifacts. Notably, we observed a temporal lag in the KvAP single-channel response to photoisomerization (Fig. 3d). Upon blue light exposure, the bilayer as an ensemble switched to the photostationary mostly-trans configuration within 1–2 ms (Fig. 1c); however, the effect was detected only after a delay of approximately 10 ms. In contrast, during the reverse transition from trans to cis upon UV light exposure, channel closure required around 40 ms.

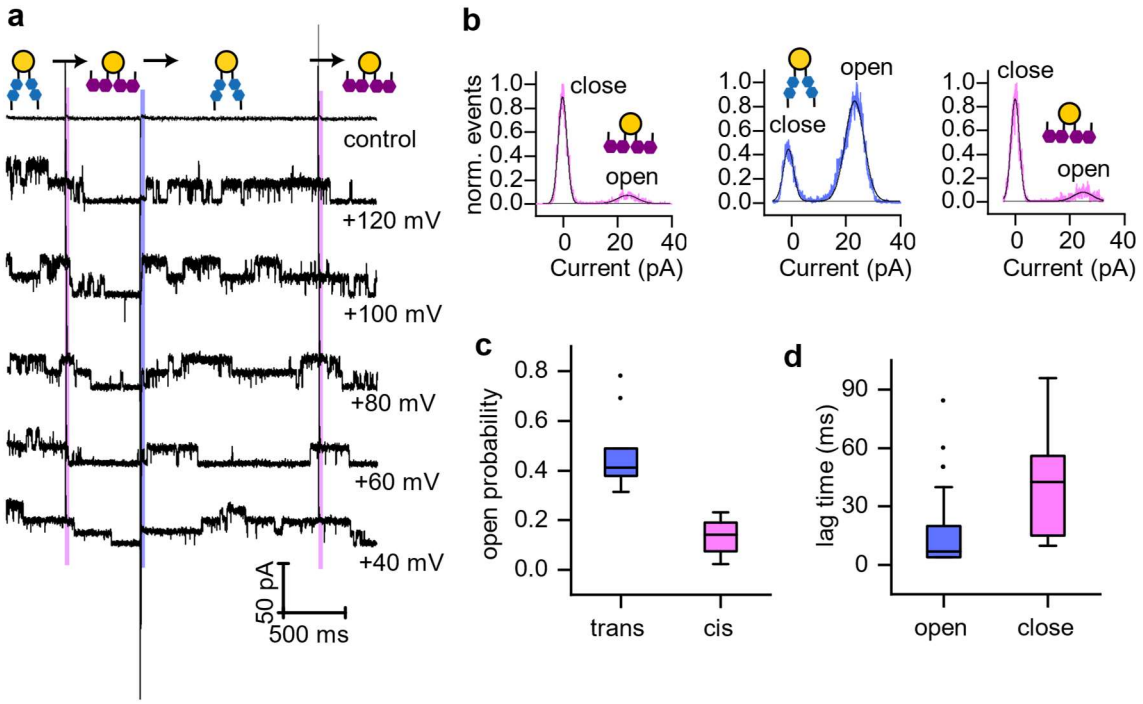

Figure 3|Modulation of KvAP single-channel activity by rapid photoisomerization of OptoDArG: (a) Representative single-channel recordings from a planar lipid bilayer (PLB) containing 20 m% OptoDArG and reconstituted KvAP channels. Recordings were conducted in 150 mM KCl, 10 mM HEPES, pH 7.4. Photoisomerization of OptoDArG was induced by 40 ms pulses of UV (magenta bars) and blue (blue bars) laser light. (b) Dwell-time histograms of KvAP single-channel activity, constructed from the recordings shown on the left. These histograms were used to calculate the P_o by determining the fraction of time at least one of the channels was in the open state. (c) Box plots illustrating P_o at an applied voltage of +120 mV for trans-OptoDArG (blue) and cis-OptoDArG (magenta). Data represent seven independent experiments for each photoisomer. (d) Lag times between OptoDArG photoisomerization and changes in channel activity: (blue) lag between cis-to-trans photoisomerization and first channel opening; (magenta) lag between trans-to-cis photoisomerization and first channel closing. Lag times were calculated from 33 channel-opening events and 34 channel-closing events.

Our single-channel experiments demonstrated that light can be used to regulate the P_o of KvAP channels. While the observed changes in P_o were modest overall, with an average increase of approximately 30%, certain experiments revealed much more pronounced effects. A striking example is shown in Figure 4, where P_o increased from ~5% to 100%. In this case, only one channel was active when OptoDArG was in its *cis* state. Upon switching to the *trans* state, five additional channels opened, resulting in a sustained increase in conductivity that did not return to baseline during the observation interval. When OptoDArG was switched back to its *cis* state, all channels but one closed after a short lag period. This variability in channel behavior complicates obtaining reliable statistics for the light-induced effects.

One consistent observation emerged from every single experiment: channel activity remained elevated for a much longer duration than it took for membrane capacitance to relax after the photo lipid was switched to its trans state. From this, we concluded that tension-related effects cannot be responsible for the increase in P_o, as tension would be expected to relax with the same time constant as membrane capacitance, i.e., within 23 ms. However, the interval between blue and UV illumination during which elevated P_o was observed exceeded 1 second. This observation aligns well with the calculated increment in tension, which was determined to be too small to significantly influence P_o.

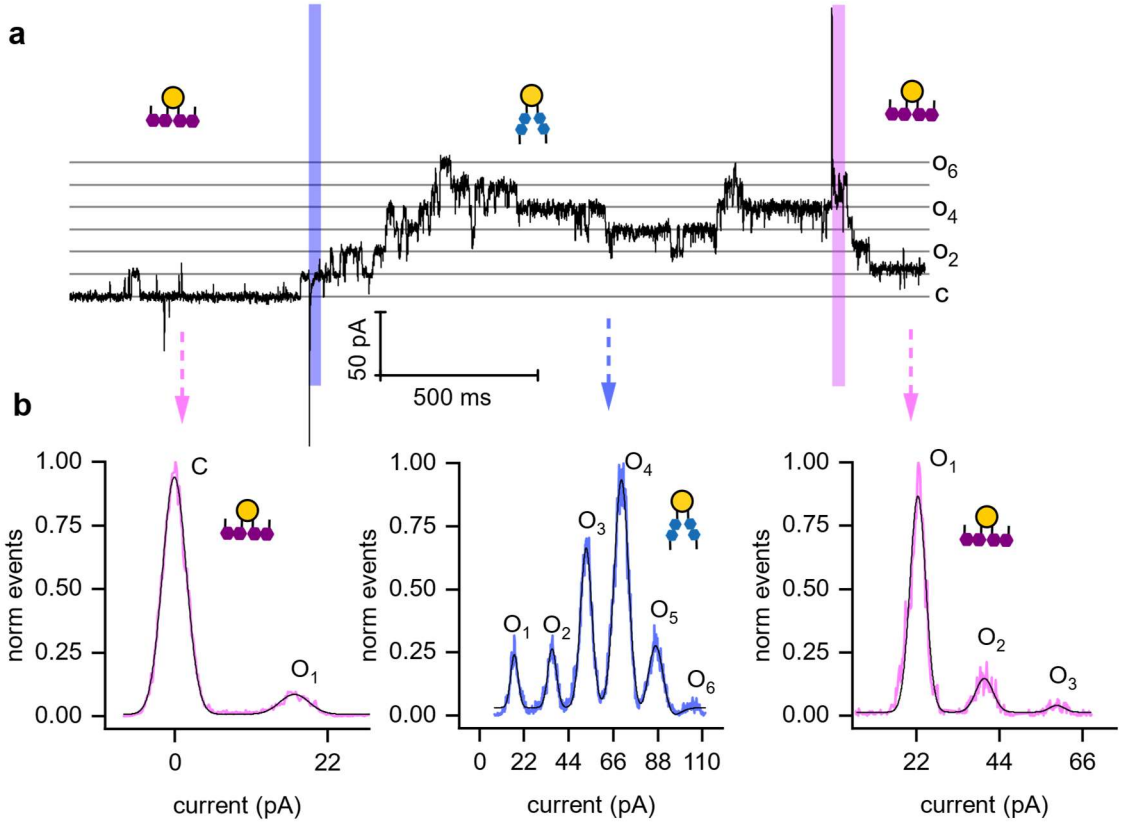

Figure 4 | Demonstration of high photoswitching efficiency: (a) Opening and closing of KvAP channels induced by illumination with blue and UV light at +100 mV. **(b)** Dwell-time histograms constructed from the recordings shown in panel (a). The experimental conditions were similar to those described in Figure 3, except for the reconstitution of a higher number of KvAP channels.

We further conducted measurements of light-modulated KvAP conductance at the ensemble level to reduce variability and improve statistical robustness (Fig. 5a). Steady-state currents recorded after the relaxation of tension under cis and trans isomer conditions (i.e., >23 ms after illumination, as shown in Fig. 1) demonstrated that in the *trans* state, where the membrane is thicker, the current was increased. This indicates that blue light induced the opening of some channels. The corresponding activity increase resulted from a leftward shift in the current-voltage dependence (Fig. 5b), consistent with the P_o changes observed in our single-channel measurements (Fig. 3).

This current modulation was reversible, as the initial current was restored by UV illumination (Fig. 5c). Specifically, in the cis state, where the membrane is thinner, a decrease in current was observed. These results confirm that photoisomerization of OptoDArG enables reversible control of K_VAP activity through alterations in bilayer properties. Notably, a modest change in capacitance of approximately 6% –

indicating an equally modest change in membrane thickness – resulted in a much larger increase in conductance (~30%).

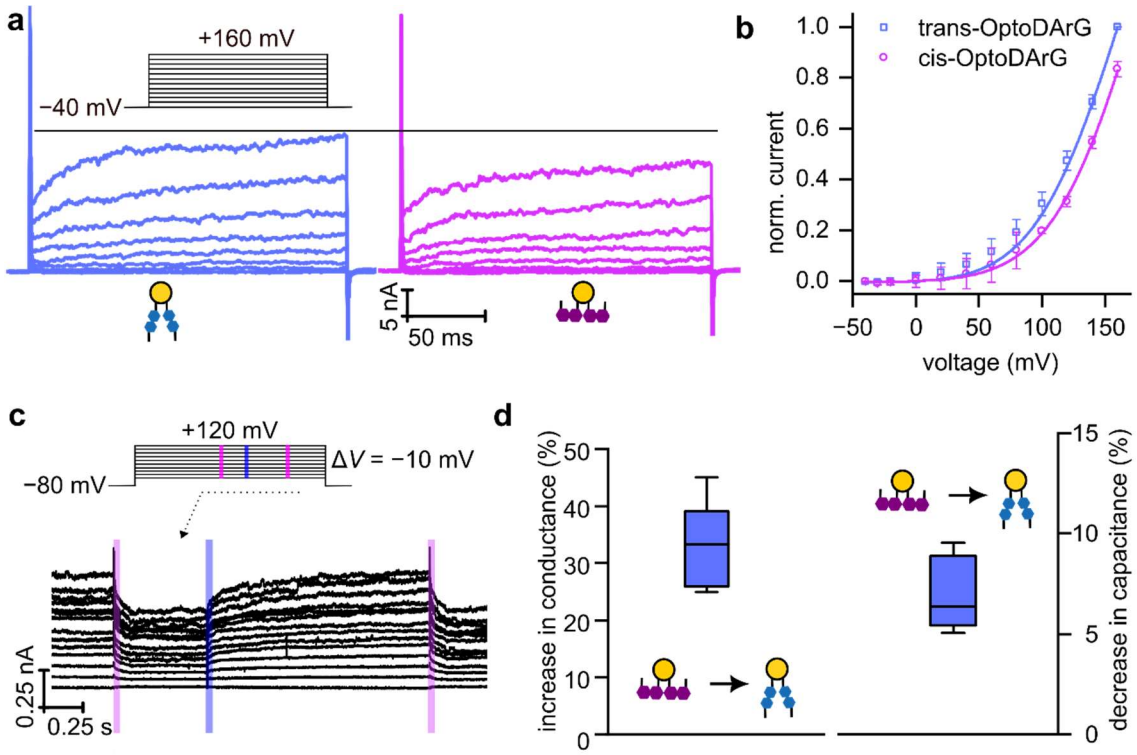

Figure 5 | Modulation of KvAP activity by photoisomerization of OptoDArG at the ensemble level. a. Voltage-dependent current recordings on a photoswitchable PLB under the same experimental conditions as in Fig. 3. The blue and magenta traces indicate recordings after membrane exposure to blue and UV laser illumination, corresponding to OptoDArG in its *trans* and *cis* states, respectively. Voltage was stepped in 20 mV increments, with pulses ranging from −40 mV to +160 mV. The inter-sweep delay was 5 s. **b.** I/V curves generated from the recordings in panel (a) (same color code) across three experimental runs. A Boltzmann function (Eq. 4) was fitted to the data (solid lines). **c.** The photoinduced increase in KvAP conductance (blue stripe) is completely reversible upon membrane exposure to a UV laser pulse (magenta stripe). Voltage was stepped in 10 mV increments, with pulses ranging from −80 mV to +120 mV. **d.** *Left panel:* A box plot showing the relative conductance increase associated with *cis* to *trans* OptoDArG conformation changes, calculated from the experiments in panels (a) and (c), and their three repetitions. *Right panel:* A box plot showing the relative decrease in steady-state capacitance measured during *cis* to *trans* OptoDArG conformation changes in the absence of KvAP (three independent experimental runs, see Fig. 1).

Discussion

Elegant cryo-electron microscopy studies have not only visualized how voltage sensors respond to an applied electric field but also revealed how these conformational changes reshape the surrounding lipid membrane.[12] We now demonstrate that the reverse phenomenon also occurs: light-induced modulation of membrane shape leads to a response of the model Kv channel KvAP. This observation indicates that the activity of Kv channels in excitable cells may be reversibly regulated by light if photoswitchable lipids are present in the plasma membrane. Importantly, this regulatory potential is versatile as it exploits alterations in a fundamental physical property – membrane thickness.

Modulation of hydrophobic membrane thickness can influence Kv's conformation due to the strong electrostatic interactions that keep the charged arginines in Kv's voltage sensors near the lipid phosphate groups. The strength of these interactions has been demonstrated in previous molecular dynamics simulations.[7-10] Consistent with our recent findings that the tilt of a transmembrane helix changes sigmoidally with membrane thickness – showing the most abrupt adjustment when the helix length and membrane thickness differ by approximately 1 nm[46] – we propose that OptoDArG's transition from the *cis* to *trans* state induces a reduction in the tilt angle of the S4 segment. This reduction repositions S4's gating charges relative to the membrane plane (Fig. 6). This movement is analogous to a (partial) "up" movement of S4 observed in a non-switchable membrane.

In a non-switchable membrane, part of the energy from the electric field must be used to locally deform the lipid. As demonstrated by cryo-EM, the local membrane thickness with an open channel exceeds that with a closed channels by ~5 Å. By pre-deforming the membrane through photoswitching, this energy expenditure is reduced. These energy savings shift the current-voltage relationship to the left (Fig. 5b). In other words, at any given voltage, we observed an increase in P_o of the Kv channels (Figs. 3–5).

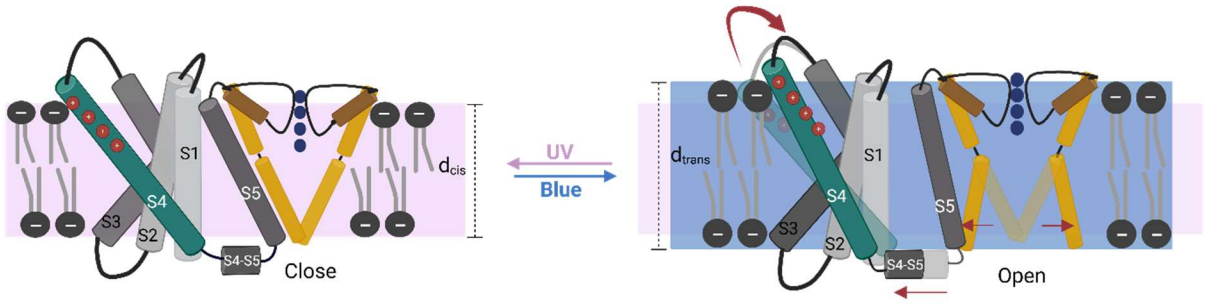

Figure 6 | Photolipid photoswitching increased the activity of voltage-sensitive potassium channels. Left panel: OptoDArG is in its *cis* state, and the channel remains closed. **Right panel:** Conversion of OptoDArG to its *trans* state thickens the membrane, inducing a change in the tilt of the S4 helix. This tilt adjustment maintains the interaction between the upper arginines (depicted as red circles) on S4 and the lipid phosphate groups. The tilt change, coupled with an "up" movement of the upper arginine, pulls the S4–S5 linker to the left. This movement propagates through S5 and the associated helix S6, enabling channel opening depending on the membrane voltage. Notably, the voltage required for channel opening is reduced.

In summary, our findings demonstrate that the voltage-driven movement of the VSD's S4 segment, and consequently the activity of KvAP and potentially other Kv channels, is influenced by membrane thickness. Membrane thickening induces a leftward shift in the current/voltage curve and may activate previously silent channels. By inducing these changes optically, our study paves the way for the use of photolipids as a novel approach to regulate the excitability of neuronal tissue.

Material and Methods

KvAP Expression and Purification

KvAP wild type was overexpressed in *E. coli* C43 (DE3) cells from a pET21a-derived expression vector. Cultures were grown in 2 L 2xYT media and induced with 1 mM isopropyl-β-D-thiogalactopyranoside (IPTG) for 4 hours. The cell pellet was resuspended in extraction buffer (basic buffer - BB: 100 mM KCl, 25 mM Tris, pH 8.0, 1 mM $MgCl_2$, and one complete protease inhibitor cocktail tablet (Roche)). Cells were lysed using an Emulsiflex homogenizer (Avestin). Cell debris was removed by centrifugation at 6,000 rpm and 4°C for 10 minutes. The membrane fraction was pelleted by ultracentrifugation at 100,000 x g and 4°C for 2 hours. The pellet was resuspended in BB containing 4% (w/v) n-decyl-β-D-maltopyranoside (DM, Anatrace) and 2 mM tris(2-carboxyethyl) phosphine (TCEP) for 2 hours at 4°C. Post-solubilization, the sample was centrifuged again at 100,000 x g and 4°C for 2 hours. The supernatant was subjected to affinity chromatography using Ni-NTA agarose (Qiagen). Purified complexes were eluted with size exclusion buffer (SE: 100 mM KCl, 25 mM Tris, pH 8.0) containing 0.25% (w/v) DM and 400 mM imidazole. Elution fractions were pooled and concentrated to a final volume of 500 µL using Pierce Protein Concentrators PES, 30 kDa MWCO, at 4,000-5,000 rpm and 4°C. Size exclusion chromatography was performed on an Äkta Pure system (Cytiva, Superdex 200 Increase 10/300 GL) to enhance purity and stability, and to remove aggregates. The concentration was determined by the Bradford method (BioRad, QuickStart Bradford 1x dye reagent), yielding 0.82 mg/mL for WT and 0.86 mg/mL for the variant. Aliquots of 50 µg protein were flash-frozen and stored at -80°C for reconstitution attempts. Ni-NTA affinity chromatography fractions and SEC fractions were analyzed by loading onto a 15% SDS-PAGE gel. Purity and oligomerization state of KvAP in the presence of SDS were assessed by Coomassie staining.

KvAP was reconstituted into *E. coli* polar lipid extract vesicles (10 mg, Avanti Polar Lipids) pre-dissolved in 0.5% (w/v) DM. Protein-to-lipid mass ratios of 1:200 and 1:50 were used. Bio-Beads SM2 (BioRad) were added to remove excess detergent, followed by overnight incubation at 4°C with gentle mixing. The suspension was then pelleted at 40,000 rpm and 4°C for 1.5 hours. The pellet was resuspended in electrophysiology buffer (EP: 10 mM HEPES, pH 7.5, 450 mM KCl, 10% (v/v) glycerol). 25 µL aliquots were flash-frozen with liquid nitrogen and stored at -80°C for subsequent experiments.

Horizontal solvent-depleted planar lipid bilayers (PLBs)

Experiments followed established procedures.[33] Lipid mixture aliquots, consisting of *E. coli* Polar Lipid Extract (PLE) and OptoDArG, were prepared in a glass vessel. The lipids were dissolved in chloroform, and the solvent was evaporated. The vessel was then flushed with argon gas and stored at −80°C.

Planar lipid bilayers (PLBs) were formed over apertures 70–100 µm in diameter in 25 µm-thick PTFE foil (Goodfellow GmbH), created using high-voltage discharge and pretreated with 0.6% hexadecane in hexane. This process utilized a custom-built PTFE chamber assembly separating two aqueous compartments. A lipid solution (10 mg/ml in hexane) was applied as monolayers to the aqueous buffer in both compartments. After hexane evaporation for >1 h (except in Fig. 1, where reduced evaporation time promoted a large torus), membrane folding was induced by rotating the upper chamber.

Successful bilayer formation was verified via capacitance measurements, with membranes exhibiting specific capacitance values >0.75 µF/cm² considered suitable for further analysis.

Optical measurement and photoisomerization

The chamber was mounted on the sample stage of an Olympus IX83 inverted microscope equipped with an iXon 897 EMCCD camera (Andor, Oxford Instruments Group). For the photoisomerization of OptoDArG-containing PLBs, a 375 nm diode laser (iBEAM-SMART-375-S, TOPTICA Photonics) was used to induce trans-to-cis conversion, and a 488 nm diode laser (iBEAM-SMART-488-S-HP, TOPTICA Photonics) was used for *cis*-to-*trans* conversion. These lasers were focused into the back-focal plane of the objective.

Controlled synchronization of the lasers, electrophysiological data acquisition, and manipulation of the motorized microscope were managed through cellSens software (Olympus) utilizing a real-time controller (U-RTC, Olympus).

Electrophysiology recordings

Following successful PLB folding, vesicles containing KvAP were added near the membrane, and fusion was facilitated via a salt concentration difference across the membrane. Vesicles were introduced to the hyperosmotic compartment with 150 mM KCl, while the hypoosmotic compartment contained 15 mM KCl. Both sides were buffered with 10 mM HEPES at pH 7.4. Voltage-clamp measurements in whole-cell

mode were made using an EPC 9 patch-clamp amplifier (HEKA Elektronik). The current was acquired at 25 kHz and analogously filtered at 10 kHz using a combination of Bessel filters. For analysis, the currents were digitally filtered at 0.5–1 kHz. Ag/AgCl salt bridges were used, and all measurements were conducted according to electrophysiological conventions, with the extracellular side of the channel taken as ground. After channel appearance, both sides of the chamber were adjusted to 150 mM KCl.

Capacitance recordings were performed using sine wave parameters for software lock-in measurements ("Sine+DC" method with computed calibration) with a 10–20 mV peak amplitude, 5 kHz frequency, 10 points per cycle, and no averaging; the voltage offset was ±10 mV.

References

1 Latorre, R. & Miller, C. Conduction and selectivity in potassium channels. *J. Membr. Biol.* **71**, 11-30 (1983).

2 Kim, D. M. & Nimigean, C. M. Voltage-gated potassium channels: a structural examination of selectivity and gating. *Cold Spring Harbor perspectives in biology* **8**, a029231 (2016).

3 Bezanilla, F. The voltage-sensor structure in a voltage-gated channel. *Trends Biochem Sci* **30**, 166-168 (2005). https://doi.org/10.1016/j.tibs.2005.02.006

4 Cha, A. & Bezanilla, F. Characterizing Voltage-Dependent Conformational Changes in the ShakerK+ Channel with Fluorescence. *Neuron* **19**, 1127-1140 (1997).

5 Armstrong, C. M. & Bezanilla, F. Charge movement associated with the opening and closing of the activation gates of the Na channels. *Journal of General Physiology* **63**, 533-552 (1974). https://doi.org/10.1085/jgp.63.5.533

6 Swartz, K. J. Sensing voltage across lipid membranes. *Nature* **456**, 891-897 (2008). https://doi.org/10.1038/nature07620

7 Freites, J. A., Tobias, D. J., Heijne, G. & White, S. H. Interface connections of a transmembrane voltage sensor. *Proceedings of the National Academy of Sciences of the United States of America* **102**, 15059-15064 (2005). https://doi.org/10.1073/pnas.0507618102

8 Schmidt, D., Jiang, Q.-X. & MacKinnon, R. Phospholipids and the origin of cationic gating charges in voltage sensors. *Nature* **444**, 775-779 (2006). https://doi.org/10.1038/nature05416

9 Krepkiy, D. *et al.* Structure and hydration of membranes embedded with voltage-sensing domains. *Nature* **462**, 473-479 (2009). https://doi.org/10.1038/nature08542

10 Chakrapani, S., Sompornpisut, P., Intharathep, P., Roux, B. & Perozo, E. The activated state of a sodium channel voltage sensor in a membrane environment. *Proceedings of the National Academy of Sciences of the United States of America* **107**, 5435-5440 (2010). https://doi.org/10.1073/pnas.0914109107

11 Sands, Z. A. & Sansom, M. S. P. How does a voltage sensor interact with a lipid bilayer? Simulations of a potassium channel domain. *Structure (London, England : 1993)* **15**, 235-244 (2007). https://doi.org/10.1016/j.str.2007.01.004

12 Mandala, V. S. & MacKinnon, R. Voltage-sensor movements in the Eag Kv channel under an applied electric field. *Proc Natl Acad Sci U S A* **119**, e2214151119 (2022). https://doi.org/10.1073/pnas.2214151119

13 Chakraborty, S. *et al.* How cholesterol stiffens unsaturated lipid membranes. *Proceedings of the National Academy of Sciences* **117**, 21896-21905 (2020).

14 Zheng, H., Liu, W., Anderson, L. Y. & Jiang, Q.-X. Lipid-dependent gating of a voltage-gated potassium channel. *Nature communications* **2**, 250 (2011). https://doi.org/10.1038/ncomms1254

15 Schmidt, D., del Marmol, J. & MacKinnon, R. Mechanistic basis for low threshold mechanosensitivity in voltage-dependent K+ channels. *Proc. Natl. Acad. Sci. U.S.A* **109**, 10352-10357 (2012). https://doi.org/10.1073/pnas.1204700109

16 Rawicz, W., Olbrich, K. C., McIntosh, T., Needham, D. & Evans, E. Effect of Chain Length and Unsaturation on Elasticity of Lipid Bilayers. *Biophys. J.* **79**, 328-339 (2000).

17 Haselwandter, C. A., Guo, Y. R., Fu, Z. & MacKinnon, R. Quantitative prediction and measurement of Piezo's membrane footprint. *Proceedings of the National Academy of Sciences* **119**, e2208027119 (2022). https://doi.org/10.1073/pnas.2208027119

18 Haselwandter, C. A., Guo, Y. R., Fu, Z. & MacKinnon, R. Elastic properties and shape of the Piezo dome underlying its mechanosensory function. *Proceedings of the National Academy of Sciences* **119**, e2208034119 (2022).

19 Wiggins, P. & Phillips, R. Analytic models for mechanotransduction: gating a mechanosensitive channel. *Proceedings of the National Academy of Sciences* **101**, 4071-4076 (2004).

20 Quemeneur, F. *et al.* Shape matters in protein mobility within membranes. *Proc. Natl. Acad. Sci. U.S.A* **111**, 5083-5087 (2014). https://doi.org/10.1073/pnas.1321054111

21 Schmidt, D. & MacKinnon, R. Voltage-dependent K+ channel gating and voltage sensor toxin sensitivity depend on the mechanical state of the lipid membrane. *Proc. Natl. Acad. Sci. U.S.A* **105**, 19276-19281 (2008). https://doi.org/10.1073/pnas.0810187105

22 Xu, Y., Ramu, Y. & Lu, Z. Removal of phospho-head groups of membrane lipids immobilizes voltage sensors of K+ channels. *Nature* **451**, 826-829 (2008). https://doi.org/10.1038/nature06618

23 Finol-Urdaneta, R. K., McArthur, J. R., Juranka, P. F., French, R. J. & Morris, C. E. Modulation of KvAP unitary conductance and gating by 1-alkanols and other surface active agents. *Biophysical journal* **98**, 762-772 (2010). https://doi.org/10.1016/j.bpj.2009.10.053

24 Saitov, A., Akimov, S. A., Galimzyanov, T. R., Glasnov, T. N. & Pohl, P. Ordered Lipid Domains Assemble via Concerted Recruitment of Constituents from Both Membrane Leaflets. *Phys. Rev. Lett.* **124**, 108102 (2020). https://doi.org/10.1103/PhysRevLett.124.108102

25 Pfeffermann, J. *et al.* Photoswitching of model ion channels in lipid bilayers. *J. Photochem. Photobiol. B: Biol.*, 112320 (2021). https://doi.org/https://doi.org/10.1016/j.jphotobiol.2021.112320

26 Bassetto, C. A. Z. *et al.* Photolipid excitation triggers depolarizing optocapacitive currents and action potentials. *Nat. Commun.* **15**, 1139 (2024). https://doi.org/10.1038/s41467-024-45403-y

27 Frank, J. A., Franquelim, H. G., Schwille, P. & Trauner, D. Optical Control of Lipid Rafts with Photoswitchable Ceramides. *J. Am. Chem. Soc.* **138**, 12981-12986 (2016). https://doi.org/10.1021/jacs.6b07278

28 Georgiev, V. N. *et al.* Area Increase and Budding in Giant Vesicles Triggered by Light: Behind the Scene. *Adv Sci (Weinh)* **5**, 1800432 (2018). https://doi.org/10.1002/advs.201800432

29 Aleksanyan, M. *et al.* Photomanipulation of Minimal Synthetic Cells: Area Increase, Softening, and Interleaflet Coupling of Membrane Models Doped with Azobenzene-Lipid Photoswitches. *Adv Sci (Weinh)* **10**, e2304336 (2023). https://doi.org/10.1002/advs.202304336

30 White, S. H. Analysis of the torus surrounding planar lipid bilayer membranes. *Biophys. J.* **12**, 432-445 (1972).

31 Sandre, O., Moreaux, L. & Brochard-Wyart, F. Dynamics of transient pores in stretched vesicles. *Proceedings of the National Academy of Sciences* **96**, 10591-10596 (1999).

32 Needham, D. & Haydon, D. A. Tensions and free energies of formation of "solventless" lipid bilayers. Measurement of high contact angles. *Biophys. J.* **41**, 251-257 (1983).

33 Horner, A., Akimov, S. A. & Pohl, P. Long and short lipid molecules experience the same interleaflet drag in lipid bilayers. *Phys. Rev. Lett.* **110**, 268101 (2013). https://doi.org/10.1103/PhysRevLett.110.268101

34 Block, S. Brownian Motion at Lipid Membranes: A Comparison of Hydrodynamic Models Describing and Experiments Quantifying Diffusion within Lipid Bilayers. *Biomolecules* **8**, 30 (2018). https://doi.org/10.3390/biom8020030

35 Cicuta, P., Keller, S. L. & Veatch, S. L. Diffusion of Liquid Domains in Lipid Bilayer Membranes. *The Journal of Physical Chemistry B* **111**, 3328-3331 (2007). https://doi.org/10.1021/jp0702088

36 Hoomann, T., Jahnke, N., Horner, A., Keller, S. & Pohl, P. Filter gate closure inhibits ion but not water transport through potassium channels. *Proc. Natl. Acad. Sci. U.S.A.* **110**, 10842-10847 (2013). https://doi.org/10.1073/pnas.1304714110

37 Aimon, S. *et al.* Functional reconstitution of a voltage-gated potassium channel in giant unilamellar vesicles. *PloS one* **6**, e25529 (2011). https://doi.org/10.1371/journal.pone.0025529

38 Ruta, V., Jiang, Y., Lee, A., Chen, J. & MacKinnon, R. Functional analysis of an archaebacterial voltage-dependent K+ channel. *Nature* **422**, 180-185 (2003). https://doi.org/10.1038/nature01473

39 Miller, C., Moczydlowski, E., Latorre, R. & Phillips, M. Charybdotoxin, a protein inhibitor of single Ca2+-activated K+ channels from mammalian skeletal muscle. *Nature* **313**, 316-318 (1985). https://doi.org/10.1038/313316a0

40 MacKinnon, R. & Miller, C. Mechanism of charybdotoxin block of the high-conductance, Ca2+-activated K+ channel. *Journal of General Physiology* **91**, 335-349 (1988). https://doi.org/10.1085/jgp.91.3.335

41 Gonzalez, C., Morera, F. J., Rosenmann, E., Alvarez, O. & Latorre, R. S3b amino acid residues do not shuttle across the bilayer in voltage-dependent Shaker K+ channels. *Proc. Natl. Acad. Sci. U.S.A* **102**, 5020-5025 (2005). https://doi.org/10.1073/pnas.0501051102

42 Tao, X. & MacKinnon, R. Functional analysis of Kv1.2 and paddle chimera Kv channels in planar lipid bilayers. *Journal of molecular biology* **382**, 24-33 (2008). https://doi.org/10.1016/j.jmb.2008.06.085

43 Zheng, H., Lee, S., Llaguno, M. C. & Jiang, Q.-X. bSUM: A bead-supported unilamellar membrane system facilitating unidirectional insertion of membrane proteins into giant vesicles. *The Journal of general physiology* **147**, 77-93 (2016). https://doi.org/10.1085/jgp.201511448

44 Aimon, S. *et al.* Functional reconstitution of a voltage-gated potassium channel in giant unilamellar vesicles. *PloS one* **6**, e25529 (2011).

45 Zheng, H., Liu, W., Anderson, L. Y. & Jiang, Q.-X. Lipid-dependent gating of a voltage-gated potassium channel. *Nat. Commun.* **2**, 250 (2011). https://doi.org/10.1038/ncomms1254

46 Kondrashov, O. V., Pinigin, K. V. & Akimov, S. A. Characteristic lengths of transmembrane peptides controlling their tilt and lateral distribution between membrane domains. *Physical Review E* **104**, 044411 (2021). https://doi.org/10.1103/PhysRevE.104.044411

Supplementary Information to

Photomodulation of Kv Channel Activity

Rohit Yadav[1,a], Juergen Pfeffermann[1,a], Nikolaus Goessweiner-Mohr[1], Toma Glasnov[2], Sergey A. Akimov[3], Peter Pohl[1,*]

[1]Institute of Biophysics, Johannes Kepler University Linz, Linz, Austria

[2]Institute of Chemistry, Karl-Franzens-University, Graz, Austria

[3]Frumkin Institute of Physical Chemistry and Electrochemistry,

Russian Academy of Sciences, Moscow, Russia

[a]These authors contributed equally

*Correspondence to: peter.pohl@jku.at

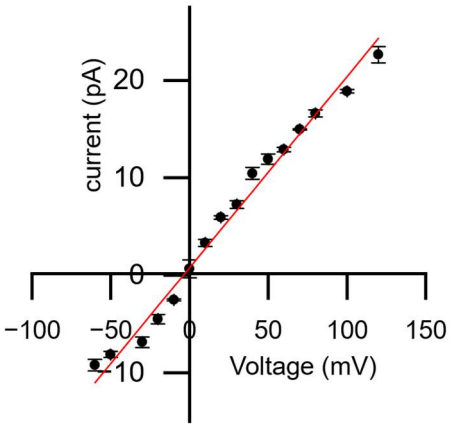

Supplementary Figure: Single-channel current of KvAP as a function of membrane voltage, recorded in photoswitchable PLBs folded from PLE with 20 m% trans-OptoDArG in 150 mM KCl, 10 mM HEPES, pH 7.4.